Biochimica et Biophysica Acta 897 (1987) 238–248
Elsevier

BBA 73384

Dynamic fluorescence quenching studies on lipid mobilities in phosphatidylcholine-cholesterol membranes

Hellmut Merkle [a], Witold K. Subczynski [b,c] and Akihiro Kusumi [a,d]

[a] *Microphotonic Center and* [b] *National Biomedical ESR Center, Department of Radiology, Medical College of Wisconsin, Milwaukee, WI 53226 (U.S.A.),* [c] *Biophysics Department, Institute of Molecular Biology, Jagiellonian University, Krakow (Poland) and* [d] *Department of Biophysics, Faculty of Science, Kyoto University, Kyoto 606 (Japan)*

(Received 1 August 1986)

Key words: Fluorescence quenching; 8-Anilinonaphthalene-1-sulfonic acid; Spin label; Cholesterol; Phospholipid membrane

Bimolecular collision rate of 8-anilinonaphthalene-1-sulfonic acid (ANS) and the nitroxide doxyl group attached to various carbons on stearic acid spin labels (*n*-SASL) in phosphatidylcholine-cholesterol membranes in the fluid phase was studied by observing dynamic quenching of ANS fluorescence by *n*-SASL's. The excited-state lifetime of ANS and its reduction by the *n*-SASL doxyl group were directly measured by the time-correlated single photon counting technique to observe only dynamic quenching separately from static quenching and were analyzed by using Stern-Volmer relations. The collision rate of ANS with the *n*-SASL doxyl group ranges between $1 \cdot 10^7$ and $6 \cdot 10^7$, and the extent of dynamic quenching by *n*-SASL is in the order of 5- $\gg$ 6- > 7- < 9- < 10- < 12- < 16-SASL (< 5-SASL) in dimyristoylphosphatidylcholine (DMPC) membranes. Collision rate of 16-SASL is only 10% less than that of 5-SASL. Since the naphthalene ring of ANS is located in the near-surface region of the membrane, these results indicate that the methyl terminal of SASL appears in the near surface area frequently, probably due to extensive *gauche-trans* isomerism of the methylene chain. The presence of 30 mol% cholesterol decreases the collision rate of ANS with 12- and 16-SASL doxyl groups but not with the 5-SASL doxyl group in DMPC membranes. On the other hand, in egg-yolk phosphatidylcholine membranes, inclusion of 30 mol% cholesterol does not affect the collision of ANS with either 5-SASL or 16-SASL doxyl groups, in agreement with our previous observation that alkyl chain unsaturation moderates cholesterol effects on lipid motion in the membrane (Kusumi et al., Biochim. Biophys. Acta 854, 307–317). It is suggested that dynamic quenching of ANS fluorescence by lipid-type spin labels is a useful new monitor of membrane fluidity that reports on various lipid mobilities in the membrane; a class of motion can be preferentially observed over others by selecting a proper spin label, i.e., rotational diffusion of lipid about its long axis and translational diffusion by using 5-SASL, wobbling motion of the lipid long axis by using 7-SASL or androstane spin label, and *gauche-trans* isomerism by using 16-SASL.

Abbreviations: ANS, 8-anilinonaphthalene-1-sulfonic acid; *n*-SASL, *n*-doxyl stearic acid spin label; DMPC, L-α-dimyristoylphosphatidylcholine; egg-yolk PC, egg-yolk phosphatidylcholine; NBD-PE, *N*-(7-nitrobenz-2-oxa-1,3-diazol-4-yl)dipalmitoyl-L-α-phosphatidylethanolamine; cholestane spin label, 3-doxyl-5α-cholestane; androstane spin label, 17β-hydroxy-4′,4′-dimethylspiro(5α-androstane-3,2′-oxazolidine)-3′-yloxyl; Tempo, 2,2,6,6-tetramethylpiperidine-1-oxyl; Tempol, 4-hydroxy-2,2,6,6-tetramethylpiperidine-1-oxyl; Tempocholine, 4-(*N*-(2-hydroxyethyl)-*N*,*N*-dimethyl)ammonium-2,2,6,6-tetramethylpiperidine-1-oxyl; Tempo-PC, Tempocholine-dipalmitoylphosphatidic acid ester.

Correspondence: A. Kusumi, Microphotonic Center, Medical College of Wisconsin, P.O. Box 26509, Milwaukee, WI 53226, U.S.A.

Introduction

Since bimolecular collision is of fundamental importance for chemical reactions, it is important in the studies of biological membranes to obtain information on dynamic structure of membranes based on bimolecular collision rate of molecule solubilized in the membrane. Kusumi et al. [1] studied bimolecular collision rate between molecular oxygen and various lipid-type spin probes in membranes by using ESR saturation recovery method. They found that oxygen transport, the product of concentration and diffusion constant of molecular oxygen, is a useful new monitor of membrane fluidity that reports on translational diffusion of small molecules in the membrane. Subczynski et al. [2] studied bimolecular collision of membrane-soluble planar copper complex and lipid spin labels in the membrane. They observed fast lateral diffusion ($(6–9.5) \cdot 10^{-7}$ cm^2/s) of the complex which is oriented along the direction of alkyl chains. The collision rate was larger in the membrane core region than in the near-surface region.

One of three major thrusts for the present paper is to expand these previous studies to bimolecular collisions of larger molecules, which are about the size of lipids, in the membrane.

Our method is based on dynamic fluorescence quenching of a fluorescence probe, 8-anilinonaphthalene-1-sulfonic acid (ANS) by the nitroxide radical attached to various carbons of the stearic acid molecule (stearic acid spin label, SASL). We made direct observation of the excited-state lifetime of ANS and its reduction (dynamic quenching) by spin labels. Dynamic quenching is different from static quenching in that the former only measures collision after the flash-light excitation while the latter reflects presence of quencher molecules within the interaction distance (4–6 Å) at the time of flash excitation. Thus dynamic quenching can be a measure of motion while static quenching reflects the spatial distribution of quenchers in the membrane. These quenching mechanisms cannot be separately observed by steady-state measurement of fluorescence because it is influenced by both dynamic and static quenching. On the other hand, lifetime measurement only detects dynamic fluorescence quenching induced by bimolecular collisions.

The use of lipid spin labels as paramagnetic quenchers has been described [3–10]. These lipid-type spin probes are particularly suitable as quenchers in membranes because their average location in the membrane has been well-characterized by a number of ESR studies (see, for example, Ref. 11). However, since most of spin-label quenching data available to date are limited to steady-state measurements, collisional effect (dynamic quenching) has not been dissociated from static quenching. We are solely concerned with dynamic quenching due to bimolecular collisions in this report. Limited application of dynamic quenching to the studies of a membrane protein [9] and lipid [7] has been reported.

One of the most important characteristics of SASL quenching is high localization of spin density of the unpaired electron in the doxyl ring [12]. Quenching would not be induced by SASL that is located adjacent to the fluorophore if the doxyl ring is away from the fluorophore. We will show that segmental motion of lipid alkyl chains (*gauche-trans* isomerism) can be estimated by using dynamic fluorescence quenching by SASL because of high localization of spin density and short interaction distances required for paramagnetic quenching.

A number of studies have been reported, in which bimolecular collision rate of lipids was estimated to obtain lateral diffusion constant of lipid molecules in the membrane by using a variety of techniques [13–20]. One of the common assumptions made to measure lateral diffusion constant by observation of bimolecular collision is that interaction probability is one when the probe molecules become adjacent to each other in the membrane [13–15, 18–20]. This assumption cannot be justified in the case of dynamic fluorescence quenching of ANS by the nitroxide spin label because interaction of ANS and the nitroxide radical may not occur during the excited-state lifetime of ANS even if ANS and SASL are adjacent to each other because the spin density of the radical is well-localized in the oxazolidine ring of SASL. The class of motion that may influence dynamic fluorescence quenching of ANS in the membrane by SASL includes (1) *gauche-trans* isomerism of lipid alkyl chains, (2) rotational dif-

fusion of SASL about its long axis, (3) wobbling diffusion of the long axis itself (SASL and fluorophores), and (4) vertical fluctuation [15] as well as (5) lateral diffusion of fluorophores and SASL (see Fig. 5). Thus, the second thrust for the present study is to develop a method of dynamic quenching of ANS fluorescence by lipid-type spin labels as a useful monitor of dynamic structure of membranes by examining closely the molecular processes that may be involved with the collision of ANS and the doxyl group of SASL.

The third thrust for this study is to examine the influence of cholesterol and alkyl chain unsaturation on bimolecular collision rate. We previously found that effects of cholesterol on lateral diffusion of phospholipids and rotational motional freedom of the nitroxide radical on 5- and 16-SASL in saturated phosphatidylcholine membranes are much greater than the cholesterol effects in unsaturated phosphatidylcholine membranes [21,22]. Unsaturation of the alkyl chains greatly reduces the ordering effect of cholesterol at C-5 and C-16 positions although unsaturation gives only minor fluidizing effects on phosphatidylcholine membranes without cholesterol; introduction of 30 mol% cholesterol to dimyristoylphosphatidylcholine (DMPC) membranes decreases the lateral diffusion of *N*-(7-nitrobenz-2-oxa-1,3-diazol-4-yl)dipalmitoyl-L-α-phosphatidylethanolamine (NBD-PE) by a factor of four at 26°C, while it causes only a slight decrease of lateral diffusion constant in dioleoylphosphatidylcholine membranes. The diffusion constant of NBD-PE in these membranes made of saturated and unsaturated phospholipids without cholesterol at 26°C is about the same, indicating little influence of unsaturated chains in the absence of cholesterol. It is interesting to re-examine these observations by monitoring bimolecular collision rates in various membranes.

Materials and Methods

All spin labels, *n*-doxyl stearic acid spin label (*n*-SASL), 3-doxyl-5α-cholestane (cholestane spin label), 17β-hydroxy-4′,4′-dimethylspiro-(5α-androstane-3,2′-oxazolidine)-3′-yloxyl (androstane spin label), 2,2,6,6-tetramethylpiperidine-1-oxyl (Tempo), 4-hydroxy-2,2,6,6-tetramethylpiperidine-1-oxyl (Tempol), and 4-(*N*-2-hydroxyethyl)-*N*,*N*-dimethyl)ammonium-2,2,6,6-tetramethylpiperidine-1-oxyl (Tempocholine chloride), and a fluorescent probe, 8-anilinonaphthalene-1-sulfonic acid (ANS) were purchased from Molecular Probes (Junction City, OR). Phospholipids were purchased from Sigma (St. Louis, MO), and cholesterol (crystallized) from Boehringer-Mannheim (Indianapolis, IN).

Some SASL contained fluorescent contamination and were purified on an activated charcoal column (0.6 × 10 cm for 10 mg of SASL in chloroform). SASL concentration after purification was determined by ESR spectroscopy. The buffer used for the study with *n*-SASL was 0.1 M borate at pH 9.5. To ensure that all SASL carboxyl groups are ionized in phosphatidylcholine membranes, a rather high pH was chosen [23–25]. Androstane spin label and cholestane spin label, which do not have any ionizable group, did not show spectral changes in phosphatidylcholine membranes between pH 4.5 and pH 9.5, indicating that the structure of phosphatidylcholine membranes is not influenced by pH in this range [1,21]. The phase transition temperature [26] and electrostatic properties [27] of phosphatidylcholine membranes are the same in this pH range. For experiments with cholestane and androstane spin labels, 0.1 M sodium *N*-2-hydroxyethylpiperazine-*N*′-2-ethanesulfonate (pH 7.4) was used as a buffer.

The membranes used in this work were multilamellar dispersions of lipids prepared in the following way: A mixture of lipid and lipid spin label in chloroform was dried with a stream of nitrogen and further dried under a reduced pressure ($\approx$ 0.1 mmHg) in the dark for at least 20 h. The suitable buffer solution was deoxygenated with nitrogen gas and mixed with an appropriate amount of concentrated ANS solution (a final concentration of 10 μM). The buffer solution (2 ml) containing ANS and the lipid samples ($2 \cdot 10^{-6}$ mol) were preheated to 37°C and then mixed vigorously with a Vortex mixer. The lipid dispersion in a test tube (4 mm i.d.) was sealed with a rubber septum and further deoxygenated by bubbling with nitrogen gas using two hypodermic needles (one for bubbling and the other for releasing the pressure). Fluorescence measurements in the test tube gave the same results as in a 10 × 10

mm quartz optical cuvette (Type 221, Hellma Cells, Inc., Jamaica, NY). All fluorescence lifetime measurements were carried out at 33.0 ± 0.5°C.

Fluorescence spectra were measured with an Aminco-Bowman SPF-500 spectrofluorometer. Time-dependent fluorescence decay after a nanosecond actinic flash light was observed by time-correlated single photon counting method using a Photochemical Research Associates Fluorescence Lifetime Instrument Type 3000 (London, Ontario, Canada). The 510C nanosecond flash lamp was filled with low-pressure hydrogen (≈ 0.5 atm) and operated at 30 KHz repetition rate. Holographic grating monochromators (Jobin-Yvon, Type H10) were set in both excitation and emission light paths with 20 nm bandwidth. Excitation and emission wavelengths were 360 nm and 460 nm, respectively. Appropriate low-cut, low-fluorescent optical filters were used to suppress second-order and stray light from the excitation monochromator and Rayleigh and Raman scattering light from the sample. The fluorescence decay curves were analyzed for multiple exponentials with deconvolution of the time-dependent lamp intensity profile using a program from Photochemical Research Associates, Inc. on a PDP 11-23 computer.

Results

Most ANS molecules partition into the membrane above the phase transition temperature. ANS fluorescence intensity is enhanced in the hydrophobic environment. The fluorescence intensity of ANS in a buffer solution in the absence of the membrane was less than 2% of that in the presence of DMPC membranes at 33°C.

ANS is reported to stay in the hydrophobic locus of the membrane close to the membrane/water interface [28] as is expected from the molecular structure, hydrophobic benzene and naphthalene rings and a sulfonyl group which is ionized under our experimental conditions. The fraction of ANS which might be located deeper in the membrane must be very small. The predominant location of ANS is confirmed by the quenching data in the latter part of this paper.

Fig. 1 shows time-dependent fluorescence decays of ANS in the presence or absence of 5-SASL

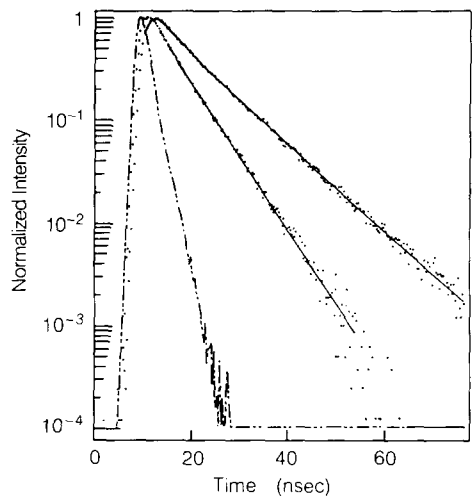

Fig. 1. Time-dependent fluorescence decays of ANS in DMPC membranes after a nanosecond flash lamp excitation at 33°C with (the faster decay) and without (the slower decay) 15 mol% 5-SASL. The lamp profile is shown in the broken line.

in DMPC membranes. Faster decays are observed in the presence of SASL in the membrane. The fluorescence decay curves can be fitted with double-exponential decays with deconvolution of the time-dependent light intensity profile of the nanosecond flash lamp. The faster decay is due to intramolecular charge transfer in the ANS molecule [29] and the slower decay is associated with a singlet-singlet electronic transition. We are concerned with reduction of the time constant of this second component by spin labels. Since we have neglected time-dependent effects in diffusion-controlled fluorescence quenching which causes departure from exponential decays [30–33], it is possible that we may be overestimating the collision rate. However, since our emphasis in this work is laid on comparison of quenching efficiency of various SASL molecules, simple analysis with multi-exponential decays were utilized in this work.

The reduction (quenching) follows the Stern-Volmer relation for dynamic quenching

$$\tau^{-1} - \tau_0^{-1} = k_q[Q]$$

where τ and τ_0 are the excited-state lifetimes in the presence and absence of quencher molecules, respectively, k_q is the kinetic constant of quench-

ing, and [Q] is the concentration of quencher molecules. In Fig. 2, $\tau^{-1} - \tau_0^{-1}$ of ANS is plotted as a function of mole fraction of 16-SASL (A) and 5-SASL (B) in DMPC membranes. These figures indicate that the Stern-Volmer equation can be used to analyze ANS quenching data with wide ranges of quencher concentrations. Structural modification of membranes with high concentration of SASL may present difficulties in interpreting the experimental data. However, $\tau^{-1} - \tau_0^{-1}$ is linear with mole fraction of *n*-SASL up to 15 mol% in these membranes. Luisetti et al. [7], in their steady-state quenching experiments, found that Stern-Volmer plot is linear up to more than 10 mol% of SASL, while London and Feigenson [8] used spin-labeled phosphatidylcholine up to 100% and found continuous changes in quenching. These results indicate that there is no transitional changes in the membrane structure upon incorporation of these spin labels to a certain level and that experimental data obtained with SASL would provide useful information for understanding the structure of membranes with and without SASL.

In the following part of this paper, we use a quenching parameter QP_{10} which is defined as an interpolated value of $\tau^{-1} - \tau_0^{-1}$ at 10 mol% of *n*-SASL, as a convenient parameter to indicate the extent of quenching.

Average location of the doxyl group of 5-SASL in the membrane is expected to be much closer to ANS than that of 16-SASL in the membrane.

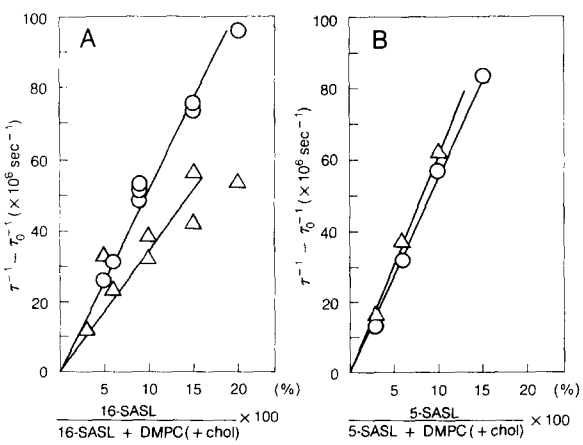

Fig. 2. $\tau^{-1} - \tau_0^{-1}$ of ANS plotted as a function of mole fraction of SASL in DMPC (○) and DMPC+30 mol% cholesterol (△) membranes at 33°C. (A) 16-SASL. (B) 5-SASL.

Comparison of Figs. 2A (16-SASL) and 2B (5-SASL), however, reveals that the collision rate of ANS with the doxyl group on 16-SASL is only 10% smaller than that of ANS and the 5-SASL doxyl group, indicating that the hydrophobic end of SASL may frequently fold back to the near-surface region of the membrane by *gauche-trans* isomerism of the alkyl chains and wobbling of the long axis (see also Fig. 3).

Influence of cholesterol (30 mol%) on dynamic quenching of ANS fluorescence by 5- and 16-SASL is also shown in Fig. 2. Inclusion of cholesterol decreases the collision rate between ANS and the doxyl ring of 16-SASL by about 30%, while it does not affect (or even slightly increases) the collision of ANS with the 5-SASL doxyl group. These results can be explained by differential effects of cholesterol on different motional modes: the presence of cholesterol may decrease the extent of *gauche-trans* isomerism, which decreases collision between ANS and the 16-SASL nitroxide, while it may not influence rotational diffusion of SASL as a hole about its long axis and thus the collision rate between 5-SASL nitroxide and ANS remains the same. The presence of 30 mol% cholesterol was previously shown to decrease lateral diffusion of NBD-PE in DMPC membranes by a factor of 4 at 26°C [21]. Since the largest effect of cholesterol on collision of ANS with SASL nitroxides observed in the present experiments was only 30% decrease in rate, it follows that lateral diffusion cannot be the rate-limiting molecular process for dynamic fluorescence quenching of ANS.

It was noted that, in $\tau^{-1} - \tau_0^{-1}$ vs. SASL-concentration plot such as those shown in Fig. 2, fluctuation of data points are larger in the presence of cholesterol and that $\tau^{-1} - \tau_0^{-1}$ tends to deviate downwardly from the linear increase above 10% SASL concentration in the membrane containing cholesterol. The error in the estimate of QP_{10} of ANS in DMPC-cholesterol membranes is larger than that in DMPC membranes due to these difficulties. Deviation from linearity may be caused by inhomogeneity, such as aggregation, of SASL in the membrane in the presence of cholesterol, which may lower the effective concentration of SASL in the membrane at higher concentrations of SASL.

The collision rate (QP_{10}) of ANS with the doxyl

group attached to various carbons on the stearyl chain is plotted as a function of location of the doxyl group in the stearyl chain in Fig. 3. QP_{10} was estimated by making a plot like those shown in Fig. 2. Fig. 3A shows QP_{10} of ANS in DMPC membranes. QP_{10} decreases steeply from C-5 to C-7 positions and increases gradually from C-9 to C-16 positions, indicating that frequency of appearance of the doxyl ring in the surface region of the membrane, where ANS is located, is larger in the methyl end portion of the stearyl chain than the middle part of the chain ($\approx$ C-7). Factors that may contribute to this observed variation in collisional quenching rate along the stearyl chain include *gauche-trans* isomerism of stearyl chains, rotational diffusion of the stearic acid about its long axis and wobbling diffusion of the long axis itself. To dissociate the effect of *gauche-trans* isomerism from that of rotation and wobbling diffusion of the long axis, we used cholestane and androstane spin labels. The structure of these spin labels implies considerably lower intramolecular motion than that of SASL and these molecules can be treated as rigid bodies in the membrane. The collision rate of ANS with the doxyl ring on these molecules should be dependent on both rotational motion about the long axis of the molecule and wobbling of the long axis, but independent of intramolecular flexibility. The result is shown in Fig. 3 (closed circle) with approximate location of the nitroxide group in the membrane: cholestane spin label places the nitroxide group near the water-membrane interface, while androstane spin label keeps the nitroxide group in the membrane at around C-10 of SASL. The collision rate of ANS with the doxyl group of androstane spin label is slightly smaller than that of 6-, 7-, 10-SASL in DMPC membranes and much smaller than that of 5-, 12-, and 16-SASL. The rates of rotational and wobbling diffusion of the long axis of androstane spin label may give an estimate for that of SASL in an approximate manner although the chemical structures of these two types of spin probes are very different. The results described above imply that wobbling diffusion of the long axis of 6-, 7-, 9-, and 10-SASL give important contribution to the collision of ANS and the doxyl group on these SASL's. Relative contribution of *gauche-trans* isomerism vs. wobbling of the long axis increases from C-10 position toward the methyl terminal of the chain. This result is in agreement with ^{2}H-NMR data [34–36], which showed that the deuterium order parameter of phospholipid alkyl chains in the membrane remains about the same between C-2 and C-10 and decreases steeply from C-10 toward the methyl end of the alkyl chain.

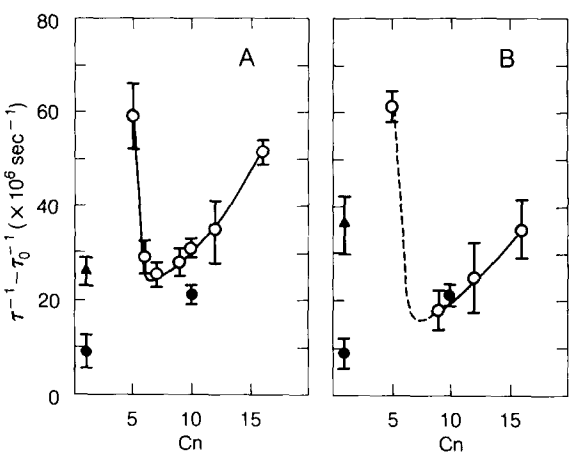

Fig. 3. QP_{10} ($\tau^{-1}-\tau_0^{-1}$ interpolated to 10 mol% of SASL in membranes) at 33°C plotted as a function of position (Cn) of the doxyl group on the stearyl chain (○), Tempo-PC (▲), and cholestane and androstane spin labels (●). (A) DMPC membranes. (B) DMPC + 30 mol% cholesterol membranes.

Blatt et al. [10] reported that the partition coefficients of SASL vary in a systematic way depending on the position of the doxyl group on the acyl chain of the fatty acid. The partition coefficient between the aqueous and egg-yolk PC membrane phases ranged between $1.2 \cdot 10^4$ and $7.4 \cdot 10^4$ at higher concentrations of SASL. According to these partition coefficients, SASL molecules incorporated into the membrane are calculated to be between 93 and 99% of the total SASL at the concentration of lipids used in this study. Thus, the variation of partition coefficient cannot explain the collision profile in the membrane shown in Fig. 3.

Quenching by cholestane spin label is small. This result can be explained by different locations of the cholestane doxyl group and the ring structures of ANS in the membrane. The nitroxide group is considerably hydrophilic and may be located in the phospholipid head-group region of the membrane. The benzene and naphthalene rings

of ANS are hydrophobic and the two rings are expected to be in the phospholipid hydrocarbon region (near the membrane surface, [28]).

Collision of ANS and the nitroxide radical is most frequent with 5-SASL. Higher collision rate of 5-SASL may be due not only to close localization of ANS and the 5-SASL doxyl group in the membrane but also fast rotational diffusion of 5-SASL about its long axis.

QP_{10} of ANS with Tempo-PC is also shown in Fig. 3. The collision rate is about half of that with 5-SASL doxyl group but is about 3-times larger than that with the doxyl group of cholestane spin label. These results suggest that the conformation of the hydrophilic head group of Tempo-PC allows access of the piperidine ring into the hydrophobic domain of the membrane between the doxyl groups of cholestane spin label and 5-SASL.

Effects of cholesterol on the collision rate (QP_{10}) of ANS with the doxyl groups on various SASL are shown in Fig. 3B as a function of location of the doxyl group on the stearyl chain. The presence of 30 mol% cholesterol in DMPC membranes decreases the collision rate of ANS with the doxyl group on 9-, 12-, and 16-SASL. This result can be explained by decreases of both *gauche-trans* isomerism and wobbling diffusion of the long axis of the stearyl chain in the presence of cholesterol. However, the collision rate of ANS with 5-SASL nitroxide was not affected (even slightly increased) by incorporation of cholesterol. It is unlikely that the cholesterol effects seen in Fig. 3B can be explained by changes in partition coefficients of SASL in the presence of cholesterol because the collision rate with 5-SASL doxyl group is not affected by the presence of cholesterol. The presence of 30 mol% cholesterol in DMPC membranes causes 30% increase in collision rate btween ANS and the spin-label piperidine ring of Tempo-PC. This result indicates larger accessibility of the phosphorylcholine headgroup to the near-surface region of the hydrophobic domain of the membrane in the presence of cholesterol. Kusumi et al. [21] previously found that incorporation of cholesterol in phosphatidylcholine membranes increases water accessibility to the interface region as monitored by cholestane spin label. These results both suggest that inclusion of cholesterol changes structural organization of headgroup regions of phospholipid membranes probably by giving extra space in the headgroup regions, which would increase the water accessibility and reduce interactions between phosphatidylcholine headgroups.

These findings and effects of alkyl chain unsaturation are summarized in Table I. Overall variation in decay constant of the slower component of ANS fluorescence examined in this study was in the range of 5 to 9 ns in the presence of 0 to 20 mol% of SASL in DMPC (DMPC + cholesterol) and egg-yolk PC (egg-yolk PC + cholesterol) membranes. The effect of cholesterol on the decay constant of ANS was small. The decay constant was reduced in the presence of unsaturated alkyl chains (egg-yolk PC membranes). Since ANS fluroescence is strongly dependent on hydrophobicity of the environment, the reduction of the lifetime may be due to increased water penetration in the membrane in the presence of unsaturated chains.

Influence of alkyl chain unsaturation on collision rate between ANS and the doxyl groups of 5- and 16-SASL is shown in Table I. Compare DMPC (which contains only saturated (myristoyl) alkyl chains) and egg-yolk PC (which contains unsaturated alkyl chains) membranes in the absence of cholesterol. QP_{10} ($\tau^{-1} - \tau_0^{-1}$ interpolated to 10 mol% of SASL) for 16-SASL is the same in DMPC and egg-yolk PC membranes. QP_{10} for 5-SASL is slightly larger (10%) in the presence of alkyl chain unsaturation (egg-yolk PC membranes). In summary, effect of alkyl chain unsaturation on the collision rate is small in phosphatidylcholine membranes without cholesterol.

TABLE I

DECAY CONSTANTS OF THE SLOWER COMPONENT AND QP_{10} AT 33°C

QP_{10}, quenching parameter at 10 mol% SASL.

Lipid	τ_0 (ns)	QP_{10} (10^6 s^{-1})	
		5-SASL	16-SASL
DMPC	9.0	57 ± 4	52 ± 4
DMPC + 30% cholesterol	9.2	62 ± 5	35 ± 8
Egg-yolk PC	7.9	64 ± 11	52 ± 9
Egg-yolk PC + 30% cholesterol	7.4	64 ± 16	58 ± 18

Compare the effect of cholesterol on DMPC and egg-yolk PC membranes in Table I. No cholesterol effect is observed on collision between ANS and the 5-SASL doxyl group either in egg-yolk PC membranes or in DMPC membranes. The colision rate of ANS and the 16-SASL doxyl group in 30% cholesterol-DMPC membranes is about 30% smaller than in DMPC membranes. This result should be contrasted with the collision rate of ANS and the 16-SASL doxyl group measured in egg-yolk PC and egg-yolk PC-cholesterol membranes. The collision rate is similar in these membranes, indicating that the influence of cholesterol observed in DMPC membranes is not present in egg-yolk PC membranes, in agreement with our previous results which showed that unsaturation of alkyl chains greatly moderates cholesterol effects on membranes [21].

Quenching of ANS fluorescence by other spin probes, Tempo, Tempol, and Tempocholine which show various solubilities in the membrane was examined to obtain more information on the location of ANS in the membrane. The molecular weights of these spin probe molecules are relatively small compared with those of phospholipids. Their solubility in membranes decreases in the order of Tempo > Tempol > Tempocholine. Fig. 4 indicates that the collision rate decreases in this order. Thus it is concluded that the naphthalene ring of ANS is located in the hydrophobic region of the membrane. The results shown in Fig. 3 are consistent with the location of the naphthalene ring between the depth of CSL and 5-SASL doxyl groups, probably a little above 5-SASL nitroxide moiety, because collision rate of ANS with 6-SASL is much smaller than that with 5-SASL.

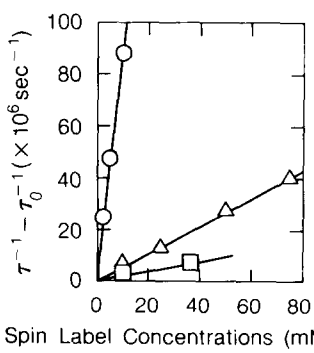

Fig. 4. $\tau^{-1} - \tau_0^{-1}$ of ANS plotted as a function of added spin label concentrations. Spin labels are Tempo (○), Tempol (△), and Tempocholine (□).

Discussion

Since information on bimolecular collision rate is important in understanding chemical reactions occurring in biological membranes, and since translational diffusion of molecules in membranes can be estimated from bimolecular collision rate, a variety of techniques have been utilized to obtain bimolecular collision rate in the membrane. These techniques can be classified on the basis of the characteristic time-scale associated with the technique which limits its sensitivity to molecular processes with comparable time constants. The characteristic time-scales of the methods using spin labels as probes, such as line broadening by spin labels [13], saturation recovery observation of collision rate with molecular oxygen [1], and electron-electron double resonance detection of collision between spin labels [14,15], are limited by T_1 (10^{-6} s) and T_2 (10^{-8} s) of spin labels. The characteristic time-scales of NMR [16], diffusion-enhanced fluorescence energy transfer of terbium and europium [17] and excimer formation of pyrene [18–20] are in the order of 10^{-1}, 10^{-3}, and 10^{-7} s, respectively. Quenching of ANS fluorescence involves the shortest time-scale among these methods because it is based on the excited-state lifetime of a fluorescence molecule ($\approx 10^{-9}$–10^{-8} s). This feature makes dynamic fluorescence quenching method unique because it is only sensitive to fast processes. Since direct observation of the excited-state lifetime and its reduction by collision with the nitroxide of spin labels (dynamic quenching) was carried out, this technique only detects motion of ANS and spin albels that makes these molecules which are outside the interaction range at the time of flash lamp excitation come into contact in the time-scale of 10^{-9}–10^{-8} s.

Translational (lateral) diffusion is the rate-limiting molecular process for bimolecular collision that is measured by other spectroscopic techniques. However, translational diffusion alone cannot explain the profile of collision between ANS and SASL in the membrane shown in Fig. 3.

In addition, translational diffusion is not sufficiently fast to explain the collision rate between ANS and 5-SASL, whose nitroxide moiety must be located at about the same depth in the membrane as the ring structures of ANS. Assuming that the mutual diffusion constant of ANS and SASL (sum of diffusion constants for ANS and SASL) is 10^{-7} cm^2/s, the range covered by the quencher molecule with respect to ANS during the excited-state lifetime of ANS is about 6 Å in radius, which is only 1.5 lipid molecules away. According to the theory developed by Träuble and Sackman [13], mutual diffusion constant of 10^{-7} cm^2/s should give QP_{10} of $1.9 \cdot 10^7$ s^{-1}. This explains only 33% of the observed collision rate between ANS and 5-SASL ($5.7 \cdot 10^7$ s^{-1}, see Table I and Fig. 3).

By using fluorescence photobleaching recovery technique, we have previously shown that the presence of 30 mol% cholesterol decreases lateral diffusion of NBD-PE in DMPC membranes by a factor of 4 at 26°C [21]. However, dynamic quenching of ANS fluorescence by the 5-SASL nitroxide was not affected (or even slightly increased) in the presence of 30 mol% cholesterol in the membrane as is shown in Figs. 2 and 3. Based on these data and the discussion in the previous paragraph, it is concluded that other molecular processes in addition to translational diffusion play key roles in determining the collision rate of ANS with the doxyl group of various SASL in the membrane.

Fig. 3 shows important contribution of *gauche-trans* isomerism to dynamic ANS fluorescence quenching. The larger effect of 16-SASL than 9-, 10- and 12-SASL may be due not only to larger probability of approach of the doxyl ring to the membrane surface but also to the larger volume swept by the 16-SASL doxyl ring during unit time.

Various types of motion that may induce dynamic fluorescence quenching of ANS are schematically summarized in Fig. 5 (tilt of alkyl chains is neglected in this figure for simplicity): (1) *gauche-trans* isomerism (G-T), (2) rotational diffusion of SASL about its long axis (R), (3) wobbling diffusion of the long axis (W), (4) vertical fluctuation (V_1, V_2), and (5) lateral diffusion (L). The mobility is shown with respect to ANS. This schematic drawing is intended to show various

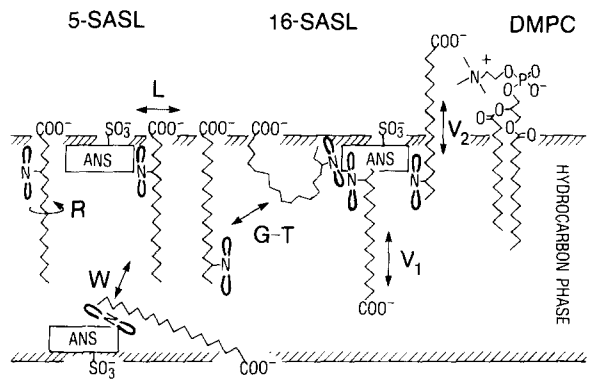

Fig. 5. Various modes of SASL motion that induce collisions of the doxyl group of SASL and ANS in DMPC membranes. G-T, *gauche-trans* isomerism: R, rotational diffusion of SASL about is long axis; W, wobbling diffusion of the long axis itself; V_1 and V_2, vertical fluctuation which transverses the bilayer (V_1) and that occurring in one side of the membrane (V_2); L, lateral diffusion.

collision mechanisms separately. In membranes, these motions are occurring simultaneously, enhancing the collision rate by combination of various mechanisms, e.g., wobbling and *gauche-trans* isomerization. Rotational diffusion of SASL about its long axis must play an important role in determining the collision rate between ANS and the 5-SASL doxyl group, while *gauche-trans* isomerism must be a critical factor for collisions between ANS and the 16-SASL doxyl group. The presence of 30 mol% cholesterol in DMPC membranes decreases *gauche-trans* isomerism of alkyl chains without changes (or even with a slight increase) in the rotational diffusion of the long axis of SASL as is shown in Fig. 3B *. Incorporation of 30

* Our data in Fig. 3 indicate that the location of ANS in the membrane is just above the 5-SASL doxyl group because the collision rate of the 6-SASL doxyl group is much smaller than that of 5-SASL and the collision rate of cholestane spin label and Tempo-PC ntiroxide groups is smaller than that of the 5-SASL doxyl group. Since the spin density on carbon and hydrogen atoms on the stearyl chain of 5-SASL is negligible except on position C-5, the collision between ANS and the 5-SASL doxyl group must be induced by motion. Rotational diffusion of 5-SASL about its long axis must be quite effective in causing quenching because the p_z orbital of the nitroxide group is extending in the direction of the membrane normal as depicted in Fig. 5. *Gauche-trans* isomerism and wobbling are not very effective in moving the doxyl group on 5-SASL toward the location of ANS.

mol% cholesterol in egg-yolk PC membranes does not change either rotational diffusion or *gauche-trans* isomerism of SASL. These results are in agreement with our previous results [21], showing that cholesterol affects phosphatidylcholine membranes with saturated alkyl chains and incorporation of unsaturation in the alkyl chain greatly moderates the effect of cholesterol.

In summary, dynamic fluorescence quenching by spin labels is shown to be a sensitive monitor of lipid mobilities in membranes. With proper selection of spin labels, it is possible to observe one class of motion preferentially over other classes of motion: rotational diffusion with 5-SASL, wobbling diffusion of the long axis with androstane spin label and 7-SASL, and *gauche-trans* isomerism with 16-SASL. Observation of dynamic quenching of ANS fluorescence by various spin labels helps to understand a variety of lipid mobilities in membranes shown in Fig. 5 in detail. By using this technique, collisional profiles across the membrane between ANS and SASL doxyl groups were obtained in DMPC and DMPC-cholesterol membranes. It is shown that the presence of 30 mol% cholesterol decreases segmental motion but not rotational motion in saturated (DMPC) membranes, and that it does not affect either segmental or rotational motion of alkyl chains in unsaturated (egg-yolk PC) membranes.

Acknowledgements

We thank Dr. James S. Hyde at the Medical College of Wisconsin and Dr. Shun-ichi Ohnishi at Kyoto University for helpful discussions and support. This work was supported in part by grants RR-01755, GM-35947, GM-22923, and RR-01008 from the National Institutes of Health of the U.S.A. and Grants-in-Aid No. 60880029 from the Ministry of Education, Science and Culture of Japan.

References

1 Kusumi, A., Subczynski, W.K. and Hyde, J.S. (1982) Proc. Natl. Acad. Sci. USA 79, 1854–1858
2 Subczynski, W.K., Antholine, W.E., Hyde, J.S. and Petering, D.H. (1986) J. Am. Chem. Soc., in the press
3 Green, J.A., Singer, L.A. and Parks, F.H. (1973) J. Chem. Phys. 58, 2690–2695
4 Bieri, V.G. and Wallach, D.F.H. (1975) Biochim. Biophys. Acta 389, 413–427
5 Bieri, V.G. and Wallach, D.F.H. (1975) Biochim. Biophys. Acta 406, 415–423
6 Bieri, V.G. and Wallach, D.F.H. (1976) Biochim. Biophys. Acta 443, 198–205
7 Luisetti, O., Mohwald, H. and Galla, H.J. (1979) Biochim. Biophys. Acta 552, 519–530
8 London, E. and Feigenson, G.W. (1981) Biochemistry 20, 1932–1938
9 Mitaku, S., Wright, J.K., Best, L. and Jähnig, F. (1984) Biochim. Biophys. Acta 776, 247–258
10 Blatt, E., Chatelier, R.C. and Sawyer, W.H. (1984) Photochem. Photobiol. 39, 477–483
11 Hubbell, W.L. and McConnell, H.M. (1971) J. Am. Chem. Soc. 93, 314–326
12 Molin, Y.N., Salikhov, K.M. and Zamaraev, K.I. (1980) Spin Exchange, pp. 19–20, Springer, New York
13 Träuble, H. and Sackmann, E. (1972) J. Am. Chem. Soc. 94, 4499–4510
14 Popp, C.A. and Hyde, J.S. (1982) Proc. Natl. Acad. Sci. USA 79, 2559–2563
15 Feix, J.B., Popp, C.A., Venkataramu, S.D., Beth, A.H., Park, J.H. and Hyde, J.S. (1984) Biochemistry 23, 2293–2299
16 Brûlet, P. and McConnell, H.M. (1975) Proc. Natl. Acad. Sci. USA 72, 1451–1455
17 Stryer, L. (1978) Annu. Rev. Biochem. 47, 819–846
18 Galla, H.-J. and Sackmann, E. (1974) Biochim. Biophys. Acta 339, 103–115
19 Galla, H.-J., Hartmann, W., Theilen, U. and Sackmann, E. (1979) J. Membrane Biol. 48, 215–236
20 Galla, H.-J. and Luisetti, J. (1980) Biochim. Biophys. Acta 596, 108–117
21 Kusumi, A., Subczynski, W.K., Pasenkiewicz-Gierula, M., Hyde, J.S. and Merkle, H. (1986) Biochim. Biophys. Acta 854, 307–317
22 Subczynski, W.K. and Kusumi, A. (1986) Biochim. Biophys. Acta 854, 318–320
23 Sanson, A., Ptak, M., Rigaud, J.L. and Gary-Bobo, C.M. (1976) Chem. Phys. Lipids 17, 435–444
24 Egret-Charlier, M., Sanson, A., Ptak, M. and Bouloussa, O. (1978) FEBS Lett. 87, 313–316
25 Kusumi, A., Subczynski, W.K. and Hyde, J.S. (1982) Fed. Proc. 41, 1394, Abstr. 6571
26 Träuble, H. and Eibl, H. (1974) Proc. Natl. Acad. Sci. USA 71, 214–219
27 Papahadjopoulos, D. (1968) Biochim. Biphys. Acta 163, 240–254
28 Podo, F. and Blasie, J.K. (1977) Proc. Natl. Acad. Sci. USA 74, 1032–1036
29 Kosower, E.M., Podiuk, H. and Kanety, H. (1978) J. Am. Chem. Soc. 100, 4179–4188
30 Ware, W.R. and Novros, J.S. (1966) J. Phys. Chem. 70, 3246–3253
31 Nemzek, T.L. and Ware, W.R. (1975) J. Chem. Phys. 62, 477–489
32 Owen, C.S. (1975) J. Chem. Phys. 62, 3204–3207

33 Vanderkooi, J.M., Fischkoff, S., Andrich, M., Podo, F. and Owen, C.S. (1975) J. Chem. Phys. 63, 3661–3666
34 Seelig, J. and Niederberger, W. (1974) J. Am. Chem. Soc. 96, 2069–2072
35 Seelig, J. and Niederberger, W. (1974) Biochemistry 13, 1585–1588
36 Stockton, G.W., Polnaszek, C.F., Leitch, L.C., Tulloch, A.D. and Smith, I.C.P. (1974) Biochem. Biophys. Res. Commun. 60, 844–850